Interactive Effects Between Aerofoils and Time Independent Flow Perturbations

A. A. F. Hashem* and R. E. Peacock†

A technique is developed to assess the interdependent effects of an aerofoil in the vicinity of, immersed in or passing through, a shear flow. The two former cases in which there is no time-dependency are analogous to an aircraft wing and slipstream combination, while the latter case may be likened to a compressor rotor blade responding to a circumferential distortion. In the model, however, no time-dependent terms are included.

A case study is made of an aerofoil of known geometry passing through a combined pressure/temperature distortion of stated initial geometry. The changes both in the streamline patterns of the distortion and of the pressure distribution are indicated and it is seen that the resulting lift response of the aerofoil bears some resemblance to that measured on rotating blades in compressors with circumferential flow conditions.

NOTATION

C	influence coefficient of γ distribution
C_L	lift coefficient
C_p	pressure coefficient
D	geometric coefficient of the aerofoil induced velocity
E	error caused by the inexact position of streamline
h	height of the aerofoil measured from the centre of the square-wave distortion (positive upwards)
L	$2L + 1$ is the number of points defining the aerofoil contour
l	length of element on the aerofoil surface‡
M	number of points on upper vortex sheet
N	number of points on lower vortex sheet
p	static pressure
P, Q	vortex sheet induced velocity derivatives
r	name of a vector (eq. 3.3)‡
s	parametric length along an aerofoil element‡
U	free stream velocity
u, v	velocity components
V	resultant velocity
w	width of the square-wave distortion
x, y	cartesian co-ordinates
z	vertical ordinate of the upper streamline
γ	vortex strength (per unit length)
η	parametric y co-ordinate along vortex sheet segment
ρ	density
ψ	stream function
ξ	parametric x co-ordinate along vortex sheet segment
ω	sheet vortex strength (per unit area)

Subscripts

I	inlet condition
a	aerofoil
af . s	aerofoil surface
i, j	point or segment indices
n	normal component
s	vortex sheet
seg	segment
o	reference conditions
∞	free stream conditions

Superscripts

$'$	field properties in the modified plane
$^-$	vector
u'	uniform flow condition

1 INTRODUCTION

An aerofoil with uniform upstream flow has a characteristic behaviour which can be predicted in incompressible conditions using techniques derived by Martensen (1) and which agree closely with experimentally derived data provided that aerofoil incidence is between the stall limits. It has however been observed that shear in the flow alters the aerofoil pressure distribution and hence lift characteristic, increasing and decreasing the lift at any incidence depending upon whether the shear component $\partial u/\partial y$ is positive or negative (2). Indeed, a circular cylinder, which is a non-lifting body in uniform flow, produces lift in a shear flow (3).

In uniform conditions the homenergic, homentropic nature of the flow simplifies the establishment of conditions around an aerofoil but shear flows create non-linear complications either by their proximity to an aerofoil or by the immersion of the aerofoil in the shear. The position is exacerbated by upwash and downwash velocities around the aerofoil which, with its immersion in the shear, alter stagnation streamline conditions in changing the position and shape of the shear flow. It is therefore recognised that, not only does the shear flow have an effect upon the aerofoil response but the aerofoil modulates the shear flow.

* Lecturer, Al-Fatah University, Tripoli, Libya.
† Senior Lecturer, The School of Mechanical Engineering, Cranfield Institute of Technology, Cranfield, Bedford, UK.
The manuscript of this paper was received on 17 January, 1979 and accepted for publication on 20 August, 1979.
‡ See Fig. (2b).

0142/727X/79/0900-0133$2.00

Numerous observations indicated that inlet flow distortions alter compressor performance and, in the instance of a circumferential distortion, since shear flows exist in the pitchwise (y) direction, it may be anticipated that a compressor blade, being the fundamental element of an axial flow compressor, will react to that shear flow. There is also likely to be an accompanied modulation of the distortion. Distortion modulation has been observed experimentally by, for example, Colpin and Kool (**4**) across a single rotor row and by Williams and Yost (**5**) in multi-stage compressors. Predictions of the change in shape of a distortion have been made by Greitzer and Strand (**6**) and by Hawthorne *et al.* (**7**). Greitzer and Strand (**6**), taking account of radial equilibrium, addressed the situation of a flow with circumferential distortion swirling in a compressor annulus. Although the rotation in the flow was created by upstream guide vanes, no blades were accounted for within the region of investigation in the annulus. Hawthorne *et al.* (**7**) allowed for the presence of blade rows in using the actuator disc assumption to resolve the non-axisymmetric flow through an annulus.

The treatment in this paper permits the presence of a real aerofoil in the region of a distortion and considers the symbiotic relationship between the aerofoil and the distortion. It ignores annular effects by considering the flow to be two-dimensional, analogous to that of a wing with a slipstream perpendicular to its profile, a two-dimensional cascade, or to a very high hub/tip ratio machine. In the solution offered the presence of one aerofoil only has been considered. This does not represent a limitation of the model but a simplification for computational purposes. Blade pitching less than the order of the width of the distortion would tend to reduce the observed effect of the aerofoil presence on the distortion. For the data presented then, the compressor analogy is that of a large pitch/chord ratio cascade ingesting a distortion of narrow pitchwise extent.

The model is quasi-steady and therefore does not represent fully the situation of a rotor passing through a distortion. A parallel model for cascades in distorted flows (**8**) has recently been applied to rotor data gained in experiment from a low speed compressor with distorted inflow (**9**) and in a stall free situation at moderate rotor speeds it is concluded that without the time-dependent terms, a good prediction of rotor behaviour results. At high rotor speeds this is not likely to be true, though. Account could nevertheless be taken of time-dependency by introducing an aerodynamic time-lag term into the calculation.

As well as evaluating the blade pressure distribution in a field containing discrete regions of shear, the method calculates the revised streamlines consequential upon the lift generated by the aerofoil. The calculated flow modulation thus becomes one component in the blade row to blade row transfer function of a distortion.

2 EQUATIONS OF FLOW

The flow is characterized as steady, but with a circumferential or pitchwise distortion and with no radial, gradients, can be regarded as two-dimensional. Assuming it to be frictionless and incompressible, the continuity and momentum equations are:

$$\frac{\partial u}{\partial x} + \frac{\partial v}{\partial y} = 0 \tag{2.1a}$$

$$u\frac{\partial \rho}{\partial x} + v\frac{\partial \rho}{\partial y} = 0 \tag{2.1b}$$

$$u\frac{\partial u}{\partial x} + v\frac{\partial u}{\partial y} = -\frac{1}{\rho}\frac{\partial p}{\partial x} \tag{2.2a}$$

$$u\frac{\partial v}{\partial x} + v\frac{\partial v}{\partial y} = -\frac{1}{\rho}\frac{\partial p}{\partial y} \tag{2.2b}$$

Equation (2.1b) is the incompressibility condition implying that the density is constant along a streamline. It may, however, vary across streamlines in the presence of a distortion created by a pressure or temperature variation.

Introducing the transformation by Yih *et al.* (**11**) a modified velocity may be defined as:

$$u' = \sqrt{\frac{\rho}{\rho_0}}\,u, \qquad v' = \sqrt{\frac{\rho}{\rho_0}}\,v \tag{2.3}$$

where ρ_0 is an arbitrarily chosen constant density. The two-dimensional field in which the flow moves at the modified velocity is identified as the modified plane. Rearranging, we obtain the modified continuity and modified momentum equation:

$$\frac{\partial u'}{\partial x} + \frac{\partial v'}{\partial y} = 0 \tag{2.1a'}$$

$$u'\frac{\partial u'}{\partial x} + v'\frac{\partial u'}{\partial y} = -\frac{1}{\rho_0}\frac{\partial p}{\partial x} \tag{2.2a'}$$

$$u'\frac{\partial v'}{\partial x} + v'\frac{\partial v'}{\partial y} = -\frac{1}{\rho_0}\frac{\partial p}{\partial y} \tag{2.2b'}$$

A stream function satisfying eq. (2.1a') is therefore given by

$$u' = \frac{\partial \psi'}{\partial y}, \qquad v' = -\frac{\partial \psi'}{\partial x} \tag{2.3'}$$

Now defining the vorticity as

$$\omega' = \frac{\partial v'}{\partial x} - \frac{\partial u'}{\partial y} \tag{2.4}$$

we get

$$\nabla^2\psi' = -\omega' \tag{2.1c}$$

$$u'\frac{\partial \omega'}{\partial x} + v'\frac{\partial \omega'}{\partial y} = 0 \tag{2.2c}$$

It is noted that although for varying density flow the vorticity is proportional to the dynamic head along every streamline, eq. (2.2c) indicates that in the modified plane the vorticity is constant along a streamline. An important implication is that the flow retains the nature of classical incompressible flow.

We thus have a generally non-linear, partial differential equation

$$\nabla^2\psi' = f(\psi')$$

3 THE MATHEMATICAL MODEL

For an unbounded linear velocity distribution the vorticity of the flow far upstream of any disturbance is constant and will remain so across the field. Use is therefore

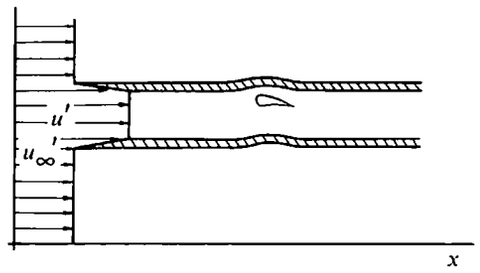

Fig. 1. The aerofoil in the modified plane

made of the Ludwig-Erickson method of representing flow who in (**12**) applied the technique to bounded regions. In the modified plane, then, the flow is approximated by regions of constant modified vorticity governed by a set of linear equations

$$\nabla^2\psi'_i = -(\omega'_\infty)_i$$

where $(\omega'_\infty)_i$ is the constant modified vorticity in the region i, any two regions are separated by a streamline initially of unknown shape.

Now if we consider a parallel flow with superimposed square-wave distortion, it is clear that, at the distortion edge, a step change in stagnation pressure with or without a temperature distortion will lead to a step change in velocity. At this discontinuity the equivalent vortex sheet will be infinite and the model will break down. To avoid this, we shall consider only square-waves with a finite edge thickness in which shear is present, thus creating in effect, a trapezoidal pattern of distortion. Such a style of distortion in any case simulates more closely a real event.

Figure 1 shows the corresponding velocity profile in the modified plane. The profile in the two edge-zones is arranged to produce a linear variation in the modified velocity. A reduction in edge zone thickness tends to reduce the importance of this restriction.

The profile of Fig. 1 can simulate several classes of distortion:

(a) a combined stagnation temperature, stagnation pressure distorted flow
(b) a constant incidence flow where at every streamline the level of temperature distortion and pressure distortion is matched to produce constant velocity from streamline to streamline.
(c) pure stagnation pressure distortion. (In the special case of both constant static and stagnation pressure the flow is potential in the modified plane. The resulting lift force remains constant irrespective of any stagnation temperature distortion).

Figure 1 shows that the flow pattern in the modified plane consists of the undisturbed velocity u'_∞ the two hatched sheets containing the area distributed, constant (same magnitude but of opposite sign) vorticity of the flow and a joining region of constant velocity u'.

For the purpose of calculation each sheet is divided into a number of segments (Fig. 2 indicates the upper sheet) although at a distance of ten to fifteen chord lengths from the aerofoil in the stream, the sheets are treated each as an undisturbed segment. The number of segments in the two sheets need not be equal. At any station i $(1 < i < M)$ the y co-ordinate of the upper and lower streamline bounding the sheet is y_i, z_i respectively.

Applying the Biot-Savart law, the vortex sheet induced velocity at any point (x, y) in the field is given by

$$u'_s(x,y) = \frac{\omega'}{2\pi}\left\{\int_{-\infty}^{x_1}\int_{y_1}^{z_1}\frac{(y-\eta)}{(x-\xi)^2+(y-\eta)^2}\,d\eta\,d\xi + \sum_{i=1}^{M-1}(u'_{seg})_i + \int_{x_M}^{\infty}\int_{y_M}^{z_M}\frac{(y-\eta)}{(x-\xi)^2+(y-\eta)^2}\,d\eta\,d\xi\right\} \tag{3.1}$$

$$v'(x,y) = -\frac{\omega'}{2\pi}\left\{\int_{-\infty}^{x_1}\int_{y_1}^{z_1}\frac{(x-\xi)}{(x-\xi)^2+(y-\eta)^2}\,d\eta\,d\xi + \sum_{i=1}^{M-1}(v'_{seg})_i + \int_{x_M}^{\infty}\int_{y_M}^{z_M}\frac{(x-\xi)}{(x-\xi)^2+(y-\eta)^2}\,d\eta\,d\xi\right\} \tag{3.2}$$

where:

$$(u'_{seg})_i = \int_{x_i}^{x_{i+1}}\int_{y(\xi)}^{z(\xi)}\frac{(y-\eta)}{(x-\xi)^2+(y-\eta)^2}\,d\eta\,d\xi$$

$$(v'_{seg})_i = \int_{x_i}^{x_{i+1}}\int_{y(\xi)}^{z(\xi)}\frac{(x-\xi)}{(x-\xi)^2+(y-\eta)^2}\,d\eta\,d\xi$$

The aerofoil is represented by a continuous vorticity distribution along its contour. This contour is defined by a number of points j $(1 < j < 2L + 1)$ with high concentration in the leading and trailing edge regions. Between any two adjacent points the vorticity γ' is assumed to vary linearly.

In vectoral form the induced velocity at any point (x, y) (lying on or outside of the aerofoil contour) due to the γ' distribution on the aerofoil is (**13**).

$$\bar{V}'_a(x,y) = \frac{1}{2\pi}\sum_{j=1}^{2L}\int_0^{l_j}\frac{\bar{r}\times\gamma'(s)\,ds\bar{k}}{r^2} \tag{3.3}$$

This can be expressed in the geometrical influence coefficient form.

$$u'_a(x,y) = \frac{1}{2\pi}\sum_{j=1}^{2L}(C_1)_j\gamma'_j + (C_2)_j\gamma'_{j+1} = \frac{1}{2\pi}\sum_{j=1}^{2L+1}(D_1)_j\gamma'_j \tag{3.4}$$

$$v'_a(x,y) = -\frac{1}{2\pi}\sum_{j=1}^{2L}(C_3)_j\gamma'_j + (C_4)_j\gamma'_{j+1} = -\frac{1}{2\pi}\sum_{j=1}^{2L+1}(D_2)_j\gamma'_j \tag{3.5}$$

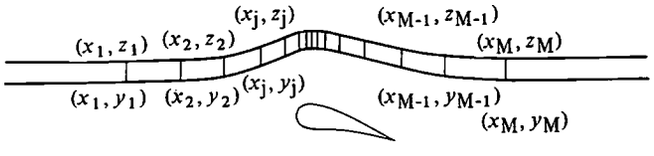

Fig. 2a. A segmented plane modified vortex sheet

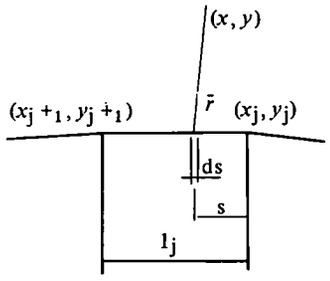

Fig. 2b. Integration nomenclature

where

$(C_2)_{j-1}, (C_4)_{j-1}$ are zero for $j = 1$
$(C_1)_j, (C_3)_j$ are zero for $j = 2L + 1$

4 METHOD OF SOLUTION

An iteration technique is necessary to gain a solution. Convergence of iteration is gained on the modified continuity eq. (2.1a) on the aerofoil surface and the four free streamlines. Iteration is dependent upon the way that the flow tangency is fulfilled at these boundaries.

Four main steps are considered and are described in more detail in Appendices.

(a) Every iteration begins with an initial assumption for the position of the free streamlines. Often, it is adequate to assume them to be unaffected by the aerofoil: however, when the aerofoil is in the vicinity of a vortex sheet or is expected to be immersed in it, an initial assumption must avoid the situation of the streamline passing through the aerofoil.

(b) The second step is to determine the vortex distribution around the aerofoil. Applying the condition of no cross-flow at the middle of elements defining the aerofoil and using the Kutta-Joukowski assumption, a solution results from the equations of the components of the aerofoil surface velocity in terms of the unknown induced effects of the vorticity distribution (γ') around the aerofoil. (Appendix A).

(c) In the third step the position of the streamlines, the only independent unknown in the problem, is adjusted (Appendix B).

At the aerofoil surface the adjustment in position of the vortex sheets produces a new vorticity distribution around the aerofoil and, feeding back to the second step, an incremental change of induced velocity at the free streamlines.

(d) The fourth step is to evaluate the lift force on the aerofoil. The static pressure distribution around the aerofoil is obtained by applying the Bernoulli equation along a streamline within a vortex sheet. It is, however, necessary to locate the stagnation streamline. To do this we may calculate the velocity profile in the region between the aerofoil and any bounding streamlines. The mass flow rate in the region is obtained by integrating the velocity profile and, knowing that the corresponding free stream velocity profile in this region is linear, we can determine the position of the stagnation streamline.

5 NUMERICAL RESULTS

For a case study a combined temperature/pressure distortion was chosen. Distortion levels were for the stagnation temperature 50° C above ambient and stagnation pressure was increased so that, in the distortion region dynamic head was 1·56 times that in undistorted flow.

The aerofoil used was of symmetrical section of 7·4 cm chord with thickness/chord ratio of 14 per cent at 35 per cent chord. The aerofoil angle of attack was maintained throughout at 4° and in the calculation the aerofoil was moved incrementally across the distortion.

Figures 3 to 9 show computer results for the location of the free streamlines and the pressure coefficient distribution around the aerofoil. All streamline plots have a

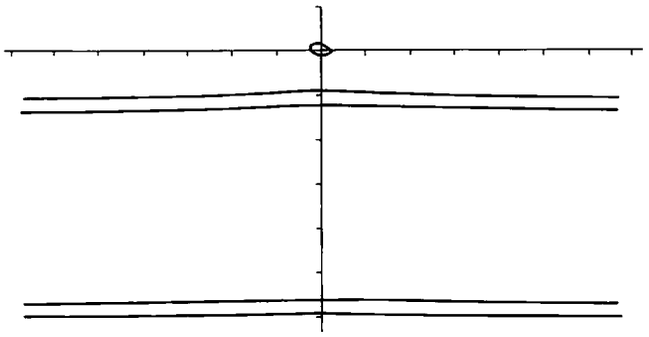

Fig. 3a. Streamline pattern with the effect of the aerofoil, $h/w = 0{\cdot}822$

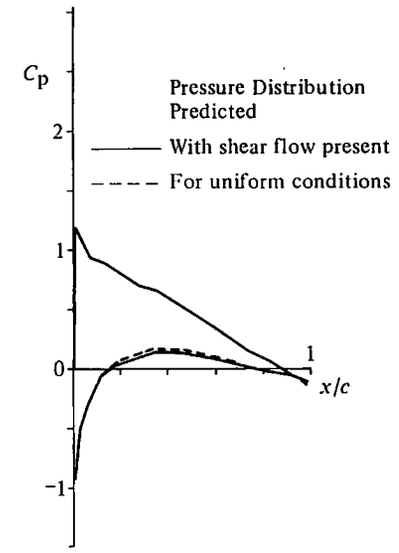

Fig. 3b. Aerofoil pressure coefficient distribution, $h/w = 0{\cdot}822$

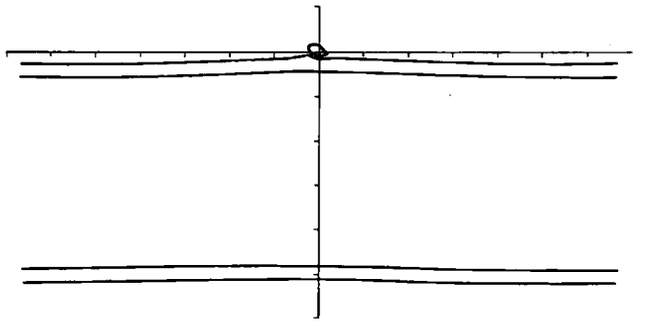

Fig. 4a. Streamline pattern with the effect of the aerofoil, $h/w = 0{\cdot}63$

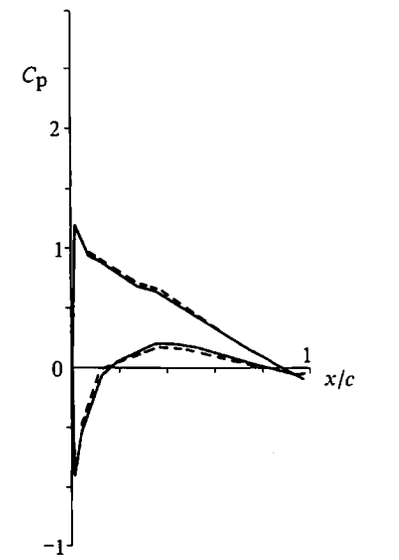

Fig. 4b. Aerofoil pressure coefficient distribution, $h/w = 0{\cdot}63$

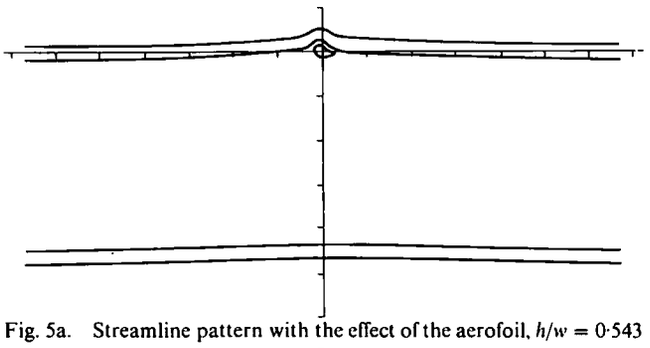

Fig. 5a. Streamline pattern with the effect of the aerofoil, $h/w = 0{\cdot}543$

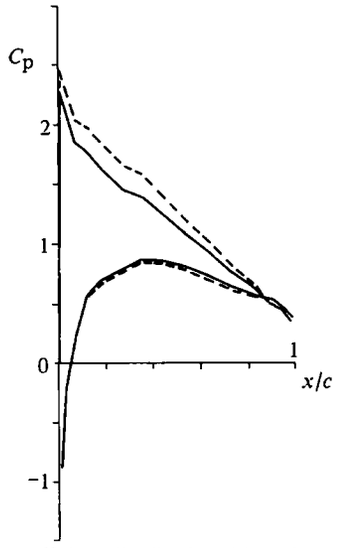

Fig. 5b. Aerofoil pressure coefficient distribution, $h/w = 0{\cdot}543$

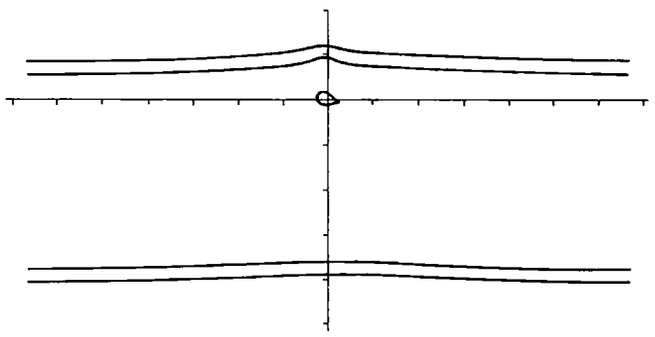

Fig. 6a. Streamline pattern with the effect of the aerofoil, $h/w = 0{\cdot}371$

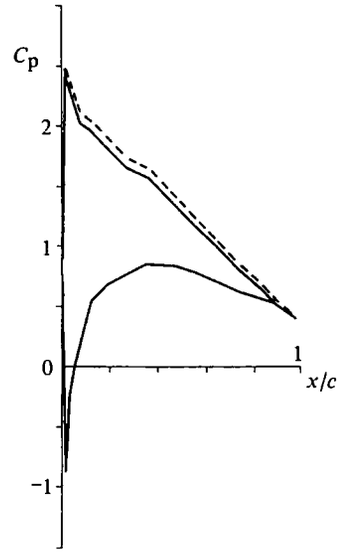

Fig. 6b. Aerofoil pressure coefficient distribution, $h/w = 0{\cdot}371$

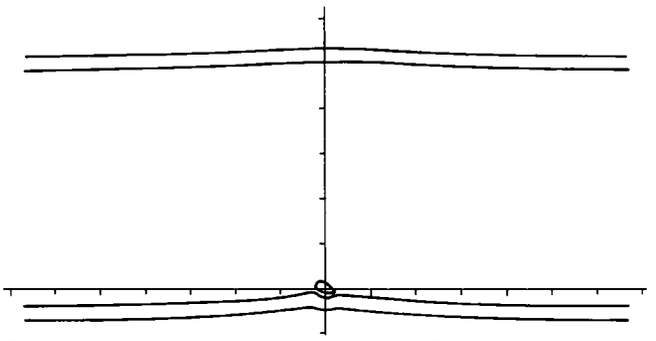

Fig. 7a. Streamline pattern with the effect of the aerofoil, $h/w = -0{\cdot}407$

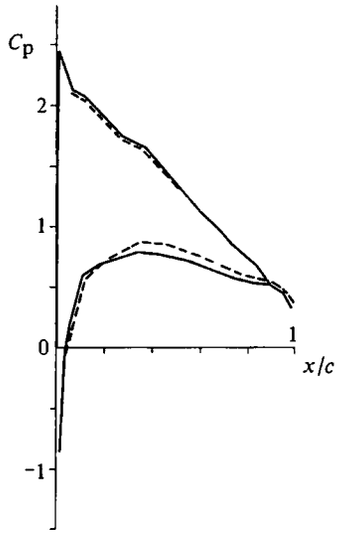

Fig. 7b. Aerofoil pressure coefficient distribution, $h/w = -0{\cdot}407$

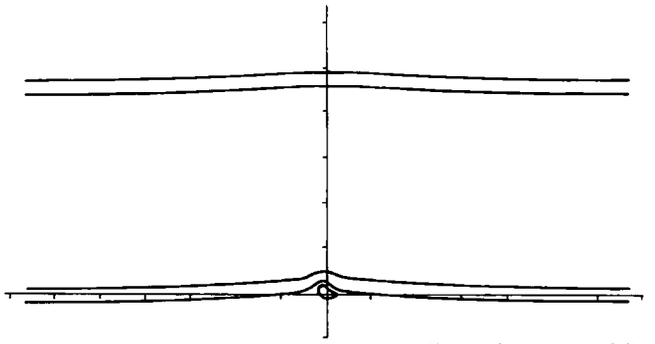

Fig. 8a. Streamline pattern with the effect of the aerofoil, $h/w = -0{\cdot}52$

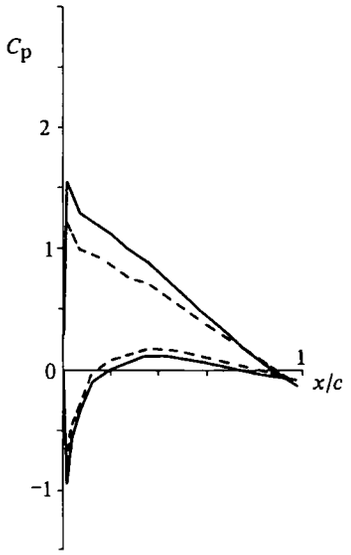

Fig. 8b. Aerofoil pressure coefficient distribution, $h/w = -0{\cdot}52$

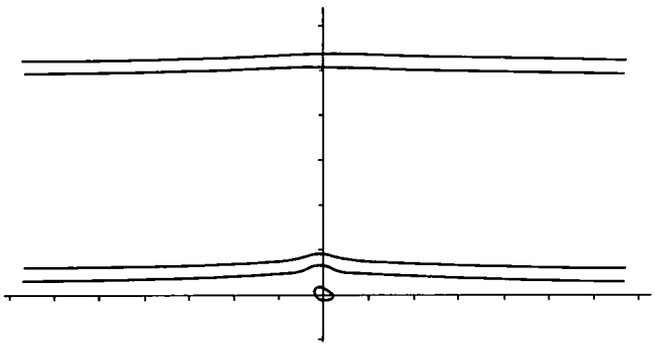

Fig. 9a. Streamline pattern with the effect of the aerofoil, $h/w = -0{\cdot}6$

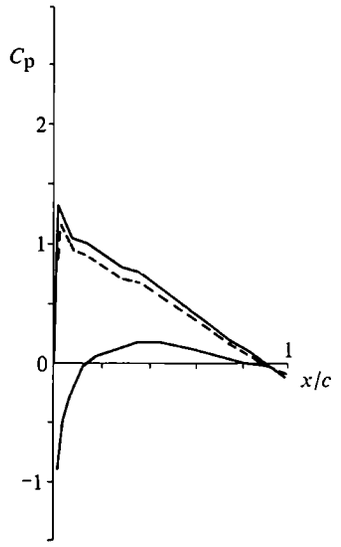

Fig. 9b. Aerofoil pressure coefficient distribution, $h/w = -0{\cdot}6$

4:1 linear magnification factor in the y' co-ordinate, resulting in magnified streamline curvature and a fat looking aerofoil. All pressure coefficient distributions are compared to that for uniform flow. The uniform flow velocity and its corresponding density were used as reference values for the dynamic head in all cases. Thus:

$$C_p = \frac{p - p_1}{(\frac{1}{2}\rho U'^2)_{h/w=-1{\cdot}2}}$$

The figures indicate that as the aerofoil approached the upper vortex sheet from either side (above or below) (Figs. 4 and 5) it experienced a lift reduction. In the vicinity of the lower vortex sheet (Figs. 7 and 8) the reverse was true, lift increasing. It may therefore be concluded that when an aerofoil is in the vicinity of vorticity whose sense is the same as that of an aerofoil circulation, the lift is increased and when in the vicinity of vorticity whose sense is in the other direction, its lift is decreased compared with uniform flow operation. This observation is confirmed by experimental results (**9**) where instrumented rotor blades in compressors were subjected to a wide range of pitchwise distortions. In the experiments described in (**9**) the distortions were all in the form of pressure decrements so that to the advancing aerofoil the distortion was recognised initially as a region of vorticity whose sense was opposite to the aerofoil lifting vortex. The resulting effect upon the aerofoil was a reduction in lift growing as the aerofoil approached the distortion. In an experiment parallel with this analytical model (**10**), a distortion seen initially by an approaching aerofoil as a vortex of the same sense as the aerofoil lifting vortex yielded at the aerofoil an increased lift, growing as the aerofoil approached the distortion. This is of course the technique of the blown flap.

Pressures on the aerofoil suction surface were consistently more sensitive to shear than those on the pressure surface: the cases shown in Figs. 4 and 5 indicate this showing more depression in the aerofoil suction surface pressure distribution with the vortex sheet passing over it than change in the pressure surface pressure distribution when the vortex sheet passed on that side of the aerofoil. This is confirmed when the aerofoil is close to the lower vortex sheet (Figs. 7 and 8). The reason for this may be seen in applying the Bernoulli equation to relate an incremental change in pressure with an incremental change in velocity:

$$\Delta p = \mp \tfrac{1}{2}\rho_0(2U'\,\Delta U' + \Delta U'^2)$$

If two incremental velocities, $\Delta U'$ equal in magnitude and induced by the vortex sheet, pass on either side of the aerofoil the effect on the suction side is magnified on account of the generally higher velocity U' on that side increasing relatively the term $2U'\,\Delta U'$.

The effect of a vortex passing the convex surface of an aerofoil is therefore larger than that for the same vortex passing the concave surface of the same aerofoil. Vortices of the same sense passing on either side of an aerofoil however have a similar effect upon the lift of the aerofoil. It may thus be concluded that an aerofoil immersed in an uniformly sheared flow, vortices of the same sense passing on either side, experiences the maximum change in lift. This particular calculation was not included in the programme, although a technique was discussed (Section 4.0) for locating the stagnation streamline when the aerofoil is in the shear region.

Considering Figs. 4 and 8 and also Figs. 5 and 7 paired respectively it is possible to establish the consequence of symmetrical types of shear flow passing an aerofoil. Figs. 4 and 8 united represent a symmetrical shear flow with a velocity decrement at the centre-line. Such a shear could be representative of the axial velocity distribution downstream of a propellor operating at part power conditions. The overall effect upon the aerofoil would be an additional lift increment, so long as the aerofoil was at an incidence or had camber. The reverse situation, in which a symmetrical distortion had its maximum velocity at the distortion centre-line, represented by uniting Figs. 5 and 7, would give an overall reduction in lift.

Integration of the pressure coefficient distributions (Figs. 3b to 9b) into a lift coefficient, non-dimensionalized in dividing by the inlet dynamic head remote from the distortion region

$$(C_L)_{h/w} = \frac{(L)_{h/w}}{(\frac{1}{2}\rho U'^2)_{h/w=-1{\cdot}2}}$$

is plotted against aerofoil position (h/w) with respect to the distortion in Fig. 10b for the distortion geometry shown in Fig. 10a. The increased lift coefficient in the distortion region reflects the locally higher velocity level which does not, in this case, appear in the denominator of the parameter. The curve then is an indication of

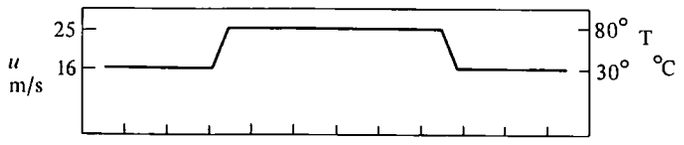

Fig. 10a. The distortion geometry

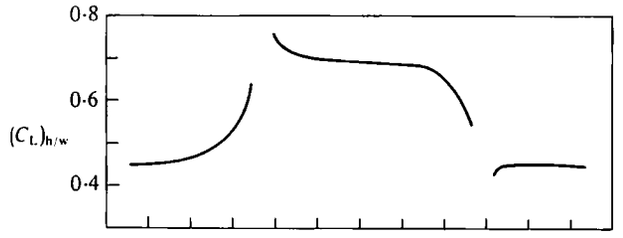

Fig. 10b. The variation of lift coefficient

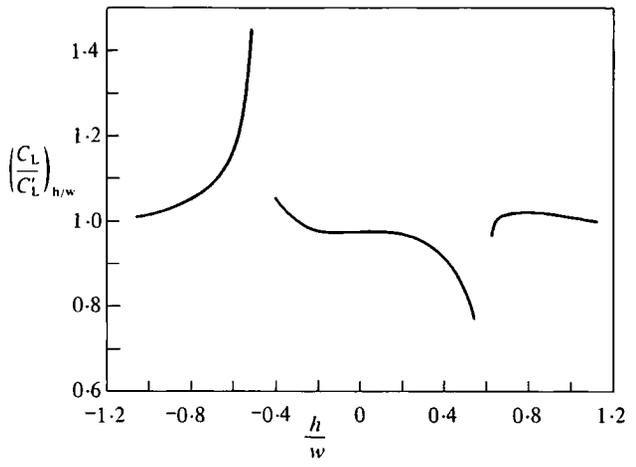

Fig. 10c. Lift coefficient compared with that for uniform flow

variation of lift experienced by the aerofoil. The effect of the high velocity level in the distortion is removed by defining a new parameter $(C_L/C'_L)_{h/w}$ where C'_L is the lift coefficient for uniform flow conditions using local inlet dynamic head. Thus, the plot of $(C_L/C'_L)_{h/w}$ (Fig. 10c) shows as a deviation from unity value the effect of shear flow only. The shear flow effect thus caused excursions in lift coefficient of between +45 per cent and −25 per cent, values which logically would be increased with the aerofoil positioned within the shear layers as discussed. The manner of fluctuation bears some resemblance to the dynamic response of rotor blades operating in distorted flow fields (**9**) but in that work, changes of rotor incidence, a consequence of the effect of a changing axial velocity, produced major excursions in lift coefficient. In addition large scale flow separations were measured in that experiment, complicating further the picture presented here. It is noted though that with favourable vorticity passing the aerofoil suction surface the aerofoil lift can be increased theoretically by as much as 45 per cent without immersion of the aerofoil in the shear flow. It may then be postulated that in an aircraft installation a gas turbine engine mounted ahead of and above the wing could result in an appreciable improvement in wing lift without the engine exhaust touching the wing structure.

The shear flow effect demonstrated in Fig. 10c is weakened as the width of the shear layer is increased, while maintaining the terminating modified velocity levels the same, effectively reducing $\partial u'/\partial y$.

Since the treatment of this paper has no time-dependency though, it might be concluded tentatively that the time-unsteady contributions to the rotor response of (**9**) is greater than at first imagined, a reinforcement of the justification, outlined in Section 1.0, for applying the quasi-steady solution to a compressor.

It may be noted that in all cases treated, no more than three iterations were ever necessary to obtain convergence of the lift coefficient within 1·5 per cent of its previous value. This value does not however represent a limitation in the model, but an arbitrarily chosen accuracy in this case for economy of computer time.

6 CONCLUSIONS

Density variation and vorticity are two major parameters in non-uniform flow fields. For two-dimensional, steady-state, low speed, non-viscous flows, the mathematical technique adopted shows that, regardless of density variations, the flow in the modified plane may be treated, by use of a velocity transformation, as classical incompressible.

A non-linear, large disturbance, mathematical model established to determine the correct location of the free streamlines, converges rapidly when the first order derivatives of the induced velocity of the two vortex sheets and the aerofoil are considered in applying the modified continuity equation.

The results of this model show the aerofoil lift coefficient to increase when the aerofoil is close to, but not necessarily immersed within, a vortex sheet whose vorticity has the same sense as the aerofoil circulation. Conversely the influence of a vortex sheet whose vorticity is in the other sense results in a reduction of aerofoil lift coefficient. A symmetrical vorticity pattern, whose components are divided by the aerofoil, produces a nett change of lift at the aerofoil, positive or negative depending upon whether the sense of the vortex passing the suction surface is of the same or opposite sense to the aerofoil lifting vortex. This arises from the observation that in all cases the aerofoil suction surface pressure distribution is more sensitive than that of the pressure surface to the proximity of a vortex sheet. These results could go some way towards explaining high lift coefficients measured on compressor rotors in distortion fields and they show that what has been considered as a non-steady response is at least partially caused by a shear flow effect without time-dependency. In an aircraft, the interactions noted could be used advantageously with a propellor/wing or gas turbine exhaust/wing combination.

ACKNOWLEDGEMENT

The work represents part of a research programme executed with support by Research Grant from the Science Research Council of Great Britain (B/RG/52028). This support is gratefully acknowledged.

REFERENCES

(1) MARTENSEN, E. 'The Calculation of the Pressure Distribution of Thick Airfoils by Means of Fredholm Integral Equations of the Second Kind'. NASA, TTF-702 July 1971

(2) BRADY, W. G., and LUDWIG, G. R. 'Aerodynamic Properties

of Airfoils in Nonuniformly Sheared Flows'. *Proc. of CAL/USAAVLABS Symposium on Aerodynamic Problems Associated with V/STOL Aircraft*, **2**, Technical Session 4 June 1966, Cornell Aeronautical Lab. Inc. Buffalo NY

(3) TSIEN, H. S. 'Symmetrical Joukowsky Aerofoils in Shear Flow', *Qu. J. App. Math.*, **1**, 130–148 (1943)

(4) COLPIN, J., and KOOL, P. 'Experimental Study of an Axial Compressor Rotor Transfer Function with Non-Uniform Inlet Flow'. *ASME Paper* 78-GT-69, Annual Gas Turbine Conference, London 1978

(5) WILLIAMS, D. D., and YOST, J. 'Some Aspects of Inlet/Engine Flow Compatibility', *J. Royal Aero. Soc.*, LXXVII, 1973

(6) GREITZER, E. M., and STRAND, T. 'Asymetric Swirling Flows in Turbomachine Annuli', Paper 78-GT-109, ASME Annual Gas Turbine Conference, London 1978

(7) HAWTHORNE, W. R., MITCHELL, N. A., McCUNE, J. E., and TAN, C. S. 'Nonaxisymmetric Flow Through Annular Actuator Discs: Inlet Distortion Problem'. Paper 78-GT-80, ASME Annual Gas Turbine Conference, London 1978

(8) EL-ATTAR, M., and PEACOCK, R. E. 'A General Solution for Distorted Flows in Cascades of Aerofoils'. *Paper* 79-GT-65, ASME Annual Gas Turbine Conference, San Diego 1979

(9) PEACOCK, R. E., and OVERLI, J. 'Dynamic Internal Flows in Compressors with Pressure Maldistributed Inlet Conditions'. *Proc. CP 177 of 46th Conf. of the AGARD PEP Panel*, Monterey, California 1975

(10) PEACOCK, R. E., and HASHEM, A. 'Stagnation Temperature and Pressure Distortion Effects upon the Response of an Aerofoil', accepted for publication in *Int. J. Heat and Fluid Flow.*

(11) YIH, C., O'DELL, W., and DEBLER, W. R. 'Prevention of Stagnation Zones in Flows of a Stratified or Rotating Fluid'. *ASME Proc. of 4th US National Cong. of App. Mech.*, **2**

(12) LUDWIG, G. R., and ERICKSON, J. C. 'Aerofoils in Two-Dimensional Non-Uniformly Sheared Slipstreams', *J. Aircraft* **8**, No. 11, Nov. 1971, 874–880

(13) STEVENS, W. A., GORADIA, S. H., and BRADON, J. A. 'Mathematical Model for Two Dimensional Multi-Component Airfoils in Viscous Flow', NASA CR-1843, July 1971, 15–32

APPENDIX A

The second step in the method of solution (Section 4.0) is to determine the vortex distribution γ' around the aerofoil.

At the aerofoil surface the velocity is given by

$$u'_a\Big|_{af.s} = u'_a(\gamma') + u'_s + U'_\infty \tag{A.1}$$

$$v'_a\Big|_{af.s} = v'_a(\gamma') + v'_s \tag{A.2}$$

Where $u'_a(\gamma')$, $v'_a(\gamma')$ are the unknown induced effects of the distribution around the aerofoil.

Applying the condition of no cross-flow at the middle of each element defining the aerofoil, $2L$ equations result. Adding the Kutta-Joukowski conditions

$$\gamma'_1 = -\gamma'_{2L+1} \tag{A.3}$$

the number of unknowns is made equal to the number of equations. Presented in matrix form we have:

$$[\gamma'] = \frac{1}{2\pi}[D]^{-1}[v'_n] \tag{A.4}$$

APPENDIX B

The third step in the method of solution (Section 4.0) is to adjust the position of the free streamlines.

Consider the lower streamline of the two vortex sheets (the same applies to the upper streamline). At an intermediate point $\bar{k}$ on the segment k of this streamline, apart from being at the exact position, the modified continuity equation in numerical difference form can be written as

$$v'(x_{\bar{k}}, y_{\bar{k}})(x_{k+1} - x_k) - u'(x_{\bar{k}}, y_{\bar{k}})(y_{k+1} - y_k) = E_{\bar{k}} \tag{B.1}$$

where

$$x_{\bar{k}} = \frac{x_{k+1} + x_k}{2}, \qquad y_{\bar{k}} = \frac{y_{k+1} + y_k}{2}$$

To obtain the correct solution we assume that at each station $i (i = 2 \to M - I,\ M + 2 \to M + N - I)$ of the two vortex sheets a vertical displacement Δy_i, Δz_i is needed for both lower and upper streamlines respectively. Considering only first order terms, the consequent incremental change in the two vortex sheets induced velocity is

$$\begin{aligned}
&\Delta u'_s(x, y + \Delta y) \\
&\quad = \sum_{i=1}^{M-1} [(Q_1)_i + (P_1)_{i-1}]\,\delta y_i \\
&\quad + \sum_{i=1}^{M-1} [(Q_2)_i + (P_2)_{i-1}]\,\delta z_i \\
&\quad + \sum_{i=M+1}^{M+N-1} [(Q_1)_i + (P_1)_{i-1}]\,\delta y_i \\
&\quad + \sum_{i=M+1}^{M+N-1} [(Q_2)_i + (P_2)_{i-1}]\,\delta z_i
\end{aligned} \tag{B.2}$$

$$\begin{aligned}
&\Delta v'_s(x, y + \Delta y) \\
&\quad = \sum_{i=1}^{M-1} [(Q_3)_i + (P_3)_{i-1}]\,\delta y_i \\
&\quad + \sum_{i=1}^{M-1} [(Q_4)_i + (P_4)_{i-1}]\,\delta z_i \\
&\quad + \sum_{i=M+1}^{M+N-1} [(Q_3)_i + (P_3)_{i-1}]\,\delta y_i \\
&\quad + \sum_{i=M+1}^{M+N-1} [(Q_4)_i + (P_4)_{i-1}]\,\delta z_i
\end{aligned} \tag{B.3}$$

where

$$(Q_1)_i = \frac{\partial (u'_{seg})_i}{\partial y_i}, \qquad (P_1)_i = \frac{\partial (u'_{seg})_{i+1}}{\partial y_{i+1}}$$

$$(Q_2)_i = \frac{\partial (u'_{seg})_i}{\partial z_i}, \qquad (P_2)_i = \frac{\partial (u'_{seg})_{i+1}}{\partial z_{i+1}}$$

$$(Q_3)_i = \frac{\partial (v'_{seg})_i}{\partial y_i}, \qquad (P_3)_i = \frac{\partial (v'_{seg})_{i+1}}{\partial y_{i+1}}$$

$$(Q_4)_i = \frac{\partial (v'_{seg})_i}{\partial z_i}, \qquad (P_4)_i = \frac{\partial (v'_{seg})_{i+1}}{\partial z_{i+1}}$$

All Q_1, Q_2, Q_3, Q_4 are equal to zero for both values of $i = 1, M + I$. Also P_1, P_2, P_3, P_4 are equal to zero for $i = M - I, M + N - I$. This follows from the assumption that at the first and last station of each vortex sheet the aerofoil induced effect is vanishing.

On the aerofoil surface the change of the two vortex sheets induced velocity will produce a new vorticity distribution around the aerofoil. The incremental change

$\Delta\gamma'$ is given by

$$[\Delta\gamma'] = \frac{1}{2\pi}[D]^{-1}\left[\sum_{i=1}^{M-1}\left(\frac{\partial v'_M}{\partial y_i}\delta y_i + \frac{\partial v'_M}{\partial z_i}\delta z_i\right) + \sum_{i=M+1}^{M+N-1}\left(\frac{\partial v'_M}{\partial y_i}\delta y_i + \frac{\partial v'_M}{\partial z_i}\delta z_i\right)\right] \quad \text{(B.4)}$$

Now we reconsider the aerofoil induced effect at points on the displaced $(\Delta y_i, \Delta z_i)$ streamlines. Ignoring second and higher order terms, it can be shown that the incremental change in the aerofoil induced velocity is

$$\Delta u'_a(x, y + \Delta y) = \frac{1}{2\pi}\sum_{j=1}^{2L+1}\left[(D_1)_j\,\Delta\gamma'_j + \gamma'_j\frac{\partial(D_1)_j}{\partial y}\delta y\right] \quad \text{(B.5)}$$

$$\Delta v'_a(x, y + \Delta y) = \frac{1}{2\pi}\sum_{j=1}^{2L+1}\left[(D_2)_j\,\Delta\gamma'_j + \gamma'_j\frac{\partial(D_2)_j}{\partial y}\delta y\right] \quad \text{(B.6)}$$

Summing up we are effectively performing a feed back loop, from the vortex sheets position to the change in the vortex distribution around the aerofoil and back to the incremental induced velocity at the streamlines. This becomes increasingly important as the aerofoil moves closer to one of the vortex sheets.

Finally we return to the previously considered point $\bar{k}$ in its new position. Combining eqs. (B.2), (B.3), (B.5) and (B.6) in the numerical difference form of the modified continuity equation we get

$$[v'(x_{\bar{k}}, y_{\bar{k}}) + \Delta v'_s(x_{\bar{k}}, y_{\bar{k}} + \Delta y_{\bar{k}}) + \Delta v'_a(x_{\bar{k}}, y_{\bar{k}} + \Delta y_{\bar{k}})] \times (x_{k+1} - x_k) - [u'(x_{\bar{k}}, y_{\bar{k}}) + \Delta u'_s(x_{\bar{k}}, y_{\bar{k}} + \Delta y_{\bar{k}}) + \Delta u'_a(x_{\bar{k}}, y_{\bar{k}} + \Delta y_{\bar{k}})](y_{k+1} - y_k + \delta y_{k+1} - \Delta y_k) = 0 \quad \text{(B.7)}$$

Manipulating equations (B.7) and (B.1) with second and higher order terms ignored, then

$$[\Delta v'_s(x_{\bar{k}}, y_{\bar{k}} + \Delta y_{\bar{k}}) + \Delta v'_a(x_{\bar{k}}, y_{\bar{k}} + \Delta y_{\bar{k}})(x_{k+1} - x_k) - u'(x_{\bar{k}}, y_{\bar{k}})](\Delta y_{k+1} - \Delta y_k) - [\Delta u'_s(x_{\bar{k}}, y_{\bar{k}} + \Delta y_{\bar{k}}) + \Delta u'_a(x_{\bar{k}}, y_{\bar{k}} + \Delta y_{\bar{k}})] \times (y_{k+1} - y_k) = -E_{\bar{k}} \quad \text{(B.8)}$$

Equation (B.8) is linear and contains all the unknown required displacements Δy_i, Δz_i $(i = 2 \to M - 1,\ i = M + 2 \to M + N - 1)$ of the four streamlines.

As the first and last segments of both the vortex sheets are located symmetrically further apart from the aerofoil (where its induced effect is vanishingly small) the modified continuity equation applied there produces two almost identical equations. Excluding one we are left with the determinate set of equations.

Having only considered first order terms throughout the derivation, the solution of the equations is not exact. Iteration proceeds until the lift force on the aerofoil is practically constant.